INTERNATIONAL JOURNAL OF CLIMATOLOGY
Int. J. Climatol. (2017)
Published online in Wiley Online Library
(wileyonlinelibrary.com) DOI: 10.1002/joc.5233

RMetS
Royal Meteorological Society

Future changes due to model biases in probabilities of extreme temperatures over East Asia using CMIP5 data

Ye-Won Seo,[a] Kyung-Sook Yun,[b†] June-Yi Lee,[b†] Yang-Won Lee,[c] Kyung-Ja Ha[a,b*] and Jong-Ghap Jhun[d]

[a] *Division of Earth Environmental System, College of Natural Science, Pusan National University, Busan, South Korea*
[b] *Research Center for Climate Sciences, Pusan National University, Busan, South Korea*
[c] *Department of Spatial Information Engineering, Pukyong National University, Busan, South Korea*
[d] *School of Earth and Environmental Sciences, Seoul National University, Seoul, South Korea*

ABSTRACT: This study examines the performances of 31 global climate models in the Coupled Model Inter-comparison Project 5 (CMIP5) in terms of probability density functions (PDFs) for maximum (*T*max) and minimum (*T*min) air temperatures over East Asia in the present and CMIP5-model projected future changes. In general, most of models well reproduce warm-season peak for both *T*max and *T*min but exhibit large inter-model spread for simulating cold-season peak, especially for *T*min. Minimum values of *T*min and *T*max are more strongly dependent upon model selection than maximum values of them. For the last 25 years of the 21st century, under the Representative Concentration Pathways 4.5 scenario, models project shifts toward warmer values in the PDFs of *T*max and *T*min and broadening in the shape of PDFs. Models with warm biases in PDFs tend to show larger shifts in temperature changes, but seasonal mean temperature biases do not affect to future changes. It is notable that the broadening of PDFs in the future influences temperature extreme events. Using the changes in probabilities of heat waves as one of extreme temperature events by comparing multi-model ensemble (MME) and models with good performance of PDFs, this study shows that MME tends to overestimate its duration. Our findings suggest that future changes in temperature extremes projected by models are strongly come from the biases detected in those models when simulating present extreme temperature PDFs. Therefore, correcting the intrinsic biases of models rather than seasonal mean correction is necessary to reduce the uncertainties in predicting future changes in temperature extremes.

KEY WORDS extreme climate; future change; East Asia; probability density function; CMIP5; heat wave

Received 6 December 2016; Revised 8 May 2017; Accepted 13 July 2017

1. Introduction

Direct and indirect effects of the observed increase in global temperature on ecosystems and human society are expected to vary considerably by region and by season. In particular, natural and human systems should be more affected by changes in climate extremes than by changes in the climatic mean state under the anthropogenic global warming (Easterling *et al.,* 2000; Tebaldi *et al.,* 2006; Zwiers *et al.,* 2011). Many previous studies have suggested that extreme climate events will become more frequent, intense and widespread in the latter half of 21st century relative to the present (Yun *et al.,* 2008; Ha and Yun, 2012; Cattiaux *et al.,* 2013; Min *et al.,* 2013; Sillmann *et al.,* 2013a; Masanganise *et al.,* 2014; Wang and Chen, 2014).

A number of researchers have examined recent changes in climate extremes over East Asia using observations and various climate extreme indices, mainly based on daily maximum (*T*max) and minimum temperature (*T*min) data (Alexander *et al.,* 2002; Zwiers *et al.,* 2011; Kharin *et al.,* 2013; Sillmann *et al.,* 2013b; Seo *et al.,* 2014). These studies have indicated that extreme heat events over East Asia have overall been increasing in magnitude and frequency under global warming in recent decades. The largest changes in percentile-based temperature indices of climate extremes reflect the frequencies of extremely cold and warm nights, which indicate a rise in minimum temperatures over Eurasia (Alexander *et al.,* 2002). In addition, the changes in mean values or variance in extreme temperatures such as *T*max and *T*min may cause the occurrence of heat waves. Climate extremes like heat waves are of great interest globally and regionally due to their high impacts on various sectors including health, agriculture, ecosystems and national economy. Recent studies suggest that heat waves are anomalous episodes with extremely high surface air temperatures, lasting for several days with serious consequences and heat-wave frequency, duration and intensity are increasing over land regions across the globe (Coumou *et al.,* 2013; Rohini *et al.,* 2016).

In addition, coupled general circulation models (CGCMs) are known for their large biases in climatology. Because many aspects of the changes in regional climate depend upon the unperturbed climatology (e.g.

* Correspondence to: K.-J. Ha, Department of Atmospheric Sciences, Pusan National University, 2, Busandaehak-ro 63beon-gil, Geumjeong-gu, Busan, 46241, South Korea. E-mail: kjha@pusan.ac.kr

†Current affiliation: IBS Center for Climate Physics, Pusan National University, Busan, South Korea.

Held and Soden, 2006; Matsueda and Palmer, 2011; Scheff and Frierson, 2012; Huang *et al.,* 2013), climatological biases in CGCMs could lead to unrealistic projections of anthropogenic climate change. However, the full importance of having an unbiased climatology for the projection of anthropogenic climate change has been insufficiently addressed and possibly underappreciated.

In addition to *T*max and *T*min, probability density functions (PDFs) of temperature are often used to explore the frequencies and severities of climate extremes (Dessai *et al.,* 2005; Alexander *et al.,* 2002; Watterson, 2008; Perkins and Pitman, 2009; Donat and Alexander, 2012; Sun *et al.,* 2015). For example, Seo *et al.* (2014) also have suggest the PDFs to evaluate the model performance in temperature over the East Asia and the best models selected by PDFs show significant increase (decrease) of summer (winter)-based extreme temperature indices. Alexander *et al.* (2002) have described a positive shift in the distribution of *T*min worldwide over 1951–2003. Boberg *et al.* (2009) used PDFs to evaluate the performances of regional climate models in projecting precipitation with climate change using daily statistics. They also reported that the shapes of the model PDFs were consistent with the shapes of the observed PDFs. The major advantage of evaluating climate models using PDFs is that PDFs can be used to demonstrate the capabilities of models to simulate values that are currently rare, but that may become more common in the future (Perkins *et al.,* 2007). As discussed by Perkins *et al.* (2007), the statistics such as means and standard deviations do not enable comparisons of the distribution of entire datasets, whereas PDFs can be used for such comparisons. Estimates of climate sensitivity made with PDFs (Andronova and Schlesinger, 2001; Forest *et al.,* 2002; Knutti *et al.,* 2002) can, therefore, be used to represent uncertainty in physical processes and feedbacks. Furthermore, a climate model's ability to simulate the complete range of observations at daily time scales can be assessed more completely using PDFs. Therefore, we have aimed to (1) evaluate the abilities of models to capture the PDFs of *T*max and *T*min over East Asia and (2) investigate future changes in extreme temperatures and their frequencies of occurrence over East Asia based on projections of the Coupled Model Inter-comparison Project 5 (CMIP5). As noted by Perkins *et al.* (2007), assessing the capacities of models to simulate climate at daily time scales is valuable because daily-scale climate directly impacts human health and activities.

This paper is structured as follows. The CMIP5 outputs and observational data used in this study and definition of heat-wave index are described in Section 2. Section 3 describes the evaluations of model performance for extreme temperatures based on PDFs for the present climate, and Section 4 describes predictions of future changes in PDFs of extreme temperature under the Representative Concentration Pathways 4.5 scenario (RCP4.5) and relationship between future changes and biases in the model based on PDFs and seasonal mean temperature. Also, future changes in heat-wave characteristics are presented. Section 5 summarizes the results and conclusions.

2. Data and method

2.1. Data and models

We use outputs for the present and future from 31 climate model simulations of the 21st century included in the CMIP5. We focus on daily extreme temperature data (i.e. *T*max and *T*min). Model evaluation is based on comparisons of the results for the period 1979–2005 between historical simulations (HIST) and data from the United States National Centres for Environmental Prediction (NCEP)/Department of Energy (DOE) Atmospheric Model Intercomparison Project (AMIP)-II reanalysis (Reanalysis-2; Kanamitsu *et al.,* 2002). Future changes are assessed based on differences in projections for the period 2075–2099 between simulations under the RCP4.5 and the HIST ensemble of simulations. Ensemble-mean assessments discussed herein use the averages of all available models. Leap years were not considered for this study. All models and observational datasets were interpolated on the $2.5° \times 2.5°$ before the analysis was performed. The East Asia region was defined as the domain within 100°–150°E and 20°–50°N. Table 1 lists the 31 CMIP5 models.

2.2. Heat-wave definition

We used the two different excess heat indices (EHIs) for identifying heat waves defined by Nairn *et al.* (2009) and Nairn and Fawcett (2015). The first one is the acclimatization index, defined as

$$\mathrm{EHI}_i\,(\mathrm{accl.}) = \left(T_i + T_{i-1} + T_{i-2}\right)/3 - \left(T_{i-3} + \ \ldots\ + T_{i-32}\right)/30$$

where T_i is the average of the *T*max and *T*min for day i. In other words, EHI_i (accl.) is the difference between the daily mean temperature (DMT) over a three-day period and the preceding 30 days. Positive values of EHI_i (accl.) represent the relatively hot weather than recent past, of excess heat, while negative values of EHI_i (accl.) denote the relatively cool weather. The second one is an absolute index, and is defined as

$$\mathrm{EHI}_i\,(\mathrm{sig.}) = \left(T_i + T_{i-1} + T_{i-2}\right)/3 - T_{95}$$

where T_{95} is the 95th percentile of T_i. We used the 27-year period 1979–2005 for the calculation of T_{95}, using all days of the year. Hence, on average T_i will exceed T_{95} on around 18 days each year. The second index called the significance index, a 3-day-averaged DMT is compared directly against the 95th percentile for DMT. Unlike EHI(accl.), this index is expected to become more extreme under a general warming trend, provided a climatological fixed period for T_{95} is adopted. If EHI(sig) is positive, then the 3-day period DMT is unusually warm with respect to the local annual climate. Conversely, if EHI(sig) is negative or zero, then the 3-day period DMT cannot be considered unusually hot, and so in order for a heat wave to be present we require EHI(sig) to be positive. Both of these two EHIs

Table 1. Summary of the CMIP5 models used in this study.

Model	Resolution	Source
ACCESS1.0	192 × 145	Commonwealth Scientific and Industrial Research Organization (CSIRO) and Bureau of Meteorology (BOM), Australia
BCC-CSM1.1	128 × 64	Beijing Climate Center (BCC), China Meteorological Administration, China
BCC-CSM1.1(m)	320 × 160	
CCSM4	288 × 192	National Center for Atmospheric Research (NCAR), USA
CESM1(BGC)	288 × 192	Community Earth System Model Contributors, USA
CESM1(CAM5)	288 × 192	
CMCC-CM	480 × 240	Centro Euro-Mediterraneo per I Cambiamenti Climatici,
CMCC-CMS	192 × 96	
CNRM-CM5	256 × 128	Centre National de Recherches Meteorologiques, France
CSIRO-Mk3.6.0	192 × 96	Australian Commonwealth Scientific and Industrial Research Organization, Australia
CanESM2	128 × 64	Canadian Centre for Climate Modelling and Analysis, Canada
FGOALS-g2	128 × 60	Institute of Atmospheric Physics (IAP), China
GFDL-CM3	144 × 90	Geophysical Fluid Dynamics Laboratory (GFDL), USA
GFDL-ESM2G	144 × 90	
GFDL-ESM2M	144 × 90	
GISS-E2-H	144 × 90	Goddard Institute for Space Studies (NASA), USA
GISS-E2-R	144 × 90	Goddard Institute for Space Studies (NASA), USA
HadGEM2-AO	192 × 145	Met Office Hadley Centre (MOHC), UK
HadGEM2-CC	192 × 145	
HadGEM2-ES	192 × 145	
INM-CM4	180 × 120	Institute for Numerical Mathematics (INM)
IPSL-CM5A-LR	96 × 96	Institut Pierre-Simon Laplace (IPSL), France
IPSL-CM5A-MR	144 × 143	
IPSL-CM5B-LR	96 × 96	
MIROC-ESM	128 × 64	Japan Agency for Marine-Earth Science and Technology, Atmosphere and Ocean Research Institute (The University of Tokyo, Japan), Japan
MIROC-ESM-CHEM	128 × 64	
MIROC5	256 × 128	Atmosphere and Ocean Research Institute, University of Tokyo, Japan
MPI-ESM-LR	192 × 96	Max Planck institute for Meteorology (MPI-M), Germany
MPI-ESM-MR	192 × 96	
MRI-CGCM3	320 × 160	Meteorological Research Institute (MRI), Japan
NorESM1-M	144 × 96	Norwegian Climate Centre (NCC), Norway

can be thought of as temperature anomalies, the first with respect to the recent past, the second with respect to the long-term climate. We then calculate the excess heat factor (EHF) as the combined effect of EHIs. The EHF is defined as follows:

$$\mathrm{EHF}_i = \max\left[1, \mathrm{EHI}_i\,(\mathrm{accl.})\right] \times \mathrm{EHI}_i\,(\mathrm{sig.})$$

where positive values of EHF_i define heat wave-like conditions for day i. Thus the EHF is an expression of the long-term temperature anomaly, amplified by the short-term temperature anomaly. It implies that a heat-wave is present if EHF is positive (but not otherwise), but if additionally the acclimatization EHI is positive, then that property amplifies its impact upon the EHF calculation. A heat wave event is considered when conditions above the criteria persist for 3 days same as a methodology adapted by Perkins and Alexander (2012). That is, EHF must be positive for at least i, $i+1$ and $i+2$. The heat waves are characterized by their duration, intensity and frequency. Using the EHF we have considered the multiple elements of heat-wave amplitude (HWA, temperature value of hottest day of hottest yearly event), their duration (HWD, length of the longest yearly event) and their frequency (HWF, yearly sum of participating heat-wave days) suggested by Fischer and Schär (2010).

3. Evaluation of east Asian extreme temperatures in the present day

3.1. PDFs of *T*max and *T*min

We compared the distributions of daily *T*max and *T*min values from the model simulations with those from observational data and used PDFs to identify potential differences between the models and observations. Figure 1 shows the PDFs of daily *T*max and *T*min averaged over East Asia with a sample size of 9855 (27 years × 365 days). Bin sizes of 0.5 °C were used for *T*max and *T*min. The PDFs exhibit two peaks associated with seasonal temperature changes from summer to winter. Hereafter, we refer to the winter peak of *T*max (*T*min) as WTX (WTN) and the summer peak of *T*max (*T*min) as STX (STN). Most models effectively reproduce the shapes of the observed PDFs for daily *T*max and *T*min, as well as the temperature peaks for both seasons. However, some models yield large discrepancies in the occurrence frequencies of each peak.

The CMIP5 Multi-Model Ensembles (MMEs) exhibit patterns very similar to those of observations; the pattern correlation coefficients between observational data and the MMEs for both *T*max and *T*min are almost equal to 0.94. To evaluate the reproduction of present *T*max and *T*min by the CMIP5 models, we calculated the pattern correlation coefficients of PDFs between observation and model output and skill scores of *T*max and *T*min (Figure 2). The performance of the models was evaluated based on a skill score defined as the inverse of the total distances between the four peaks in PDFs from a model and those from observational data. Total distances are calculated by square root of sum of temperature and frequency difference between observation and models at all peaks. Therefore, a larger skill score indicates good performance of the simulation for the present climate, which corresponds to a good match between observations and model outputs at the four peaks. In addition, 21 models among 31 models used in this study (68% of the total number of models), *T*max of model outputs shows stronger correlation with observed data than *T*min. Although *T*max captures the distribution of frequency and temperature at each peak more effectively than does *T*min, the correlation coefficients for MMEs of *T*min are as high as those of *T*max because the means between models of the two groups overestimate and underestimate frequencies for WTN. The large biases in WTN for each model have substantial impacts for projecting future temperature changes. It indicates that future projection for winter extreme should have larger uncertainty than summer counterpart. We also identified the five best models based on higher skill score above 0.5: BCC-CSM1−1-M, CESM1-BGC, CMCC-CMS, HadGEM2-AO and MPI-ESM MR; these models also yielded high pattern correlation coefficients above 0.85. Hereafter, we refer these best five models' MME as a best-multi model ensemble (BMME). We note that the CMIP5 models reproduce the annual distributions of present-day *T*max and *T*min over East Asia reasonably well.

3.2. Extreme temperature events

We investigated annual extreme temperatures and their dates of occurrence in the observational data and HIST, as shown in Figure 3. The day with the lowest value of *T*max in a year represents the day that was coldest during daytime, and the day with the highest temperature of *T*max in a year represents the day that was hottest during daytime which can be considered the Hot Days. In the observed data and the MMEs, the dates that were coldest during daytime were January 15 and 18, with temperatures of 1.1 and 3.4 °C. The MMEs thus show a warm bias in the extreme cold *T*max values (2.3 °C warmer) with a 3-day delay in occurrence compared to observations. The observed date of the maximum of *T*max is similar to that of MMEs; these dates are August 1 and 3, with temperature of 27.2 and 25.4 °C, respectively.

The date of the lowest temperature of *T*min in a year represents the coldest day of the year during early morning; such days are considered to as the Frost Days. The dates of the minimum of *T*min from observations and from MMEs are January 21 and 22, with temperatures of −4.7 and −2.8 °C, respectively. It is notable that the minimum *T*min events occur about 1 week later than the minimum *T*max events. The day with the highest temperature day of *T*min in a year is regarded as the hottest day during nighttime; such days can be considered as Tropical Nights. The dates of the maximum of *T*min based on the observational data and MME are July 31 and August 2, and theirs temperature are 21.8 and 20.2 °C. Most of models capture well the dates of these extreme events because of their good performance in simulating the annual cycles (not shown). The inter-model spread for the occurrence dates of all extreme events is 9.03−11.15 days. If two models having poor projection of the annual cycle (MIROC-ESM and MIROC-ESM-CHEM) are excluded, the variance in the occurrence dates of the extreme events is reduced to about 4.13−5.48 days. These two models do affect date variance but do not affect temperature variance. Compared to the maximum events of extreme temperatures, the minimum events have large discrepancies in temperatures and dates of occurrence. This finding is consistent with the suggestion of Kharin *et al.* (2007) that model discrepancies in simulating cold extremes are generally larger than those in simulating warm extremes. Overall, the simulation of extreme nighttime events is more model-dependent than that of extreme of daytime events.

4. Future changes under the RCP4.5 scenario

4.1. PDFs for *T*max and *T*min

We have investigated the PDFs for *T*max and *T*min for the period of 2075−2099 under the RCP4.5 scenario (Figure 4). In general, the shapes of the model-based PDFs for *T*max and *T*min under RCP4.5 are consistent with the shapes of the PDFs from HIST with a little broadening, having a horizontal shift toward higher values appears in PDFs for all models compared to those for the HIST results. The MMEs project that the peak values of the PDFs for *T*max and *T*min will shift 2.0 to 3.0 °C higher in the future under RCP4.5. Compare to results of present climate in Figure 1, inter-model spread of temperature increases at all peaks. Whereas the MMEs present lower frequencies of occurrence at all peaks, and these changes due to the increase of inter-model spread of the frequencies of occurrence. The clear increase in the uncertainty of future temperature projections is notable. Some models (IPSL-CM4B-LR, inmcm4 and HadGEM2-ES) show decreases of lower peak temperatures in *T*max and *T*min than those of MME for HIST.

4.2. Sensitivity of temperature change probabilities

To examine the changes associated with biases in temperature, we present responses to the temperature biases at the four peaks (Figure 5). In general, the temperature changes and biases show linear relationships with high correlation coefficients: above 0.82 at all peaks. The strongest

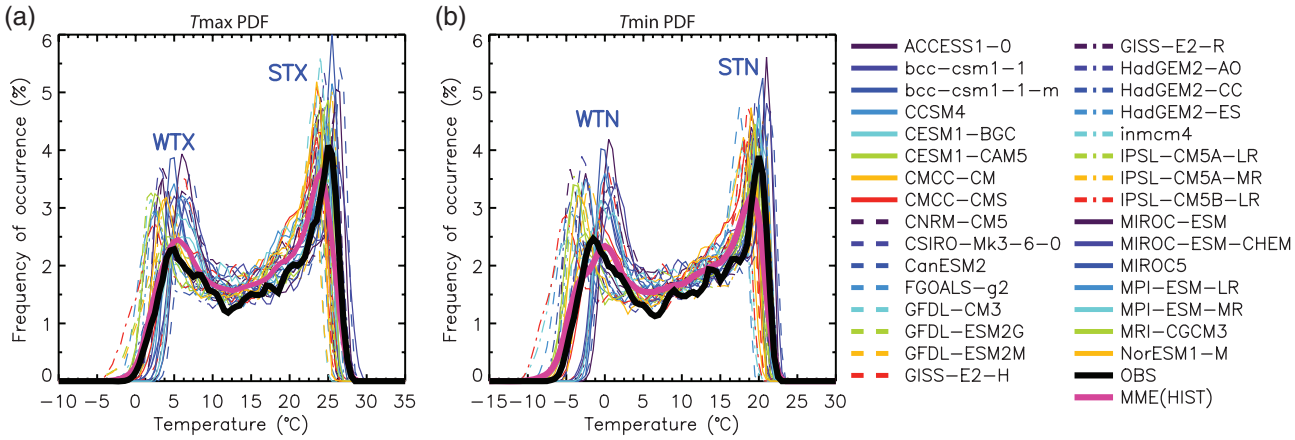

Figure 1. The probability density functions (PDFs) of annual daily (a) maximum temperatures and (b) minimum temperatures over East Asia (100°–150°E, 20°–50°N) for 1979–2005 in HIST. The black and pink curves denote the observational data and MMEs in HIST, respectively. [Colour figure can be viewed at wileyonlinelibrary.com].

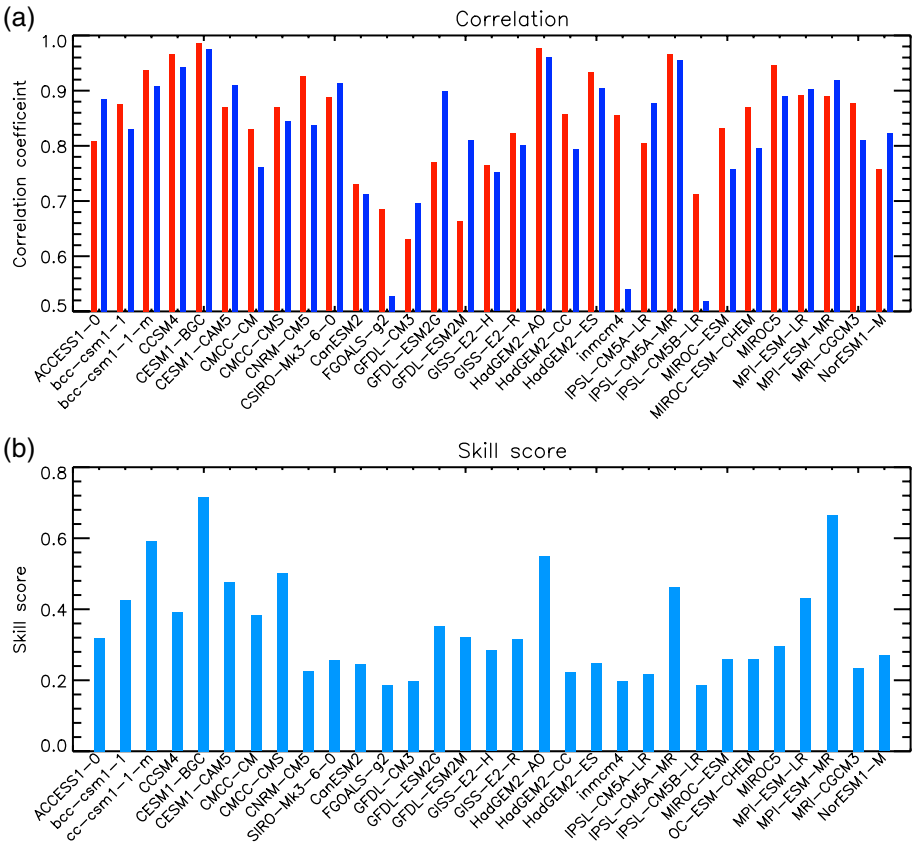

Figure 2. (a) The pattern correlation coefficients of PDFs between observational data and model outputs in HIST and (b) skill scores for projections of maximum temperature and minimum temperature. The red and blue bars in figure (a) represent maximum temperatures and minimum temperatures, respectively. [Colour figure can be viewed at wileyonlinelibrary.com].

relationship occurs with the winter peak of *T*min, as indicated by its high correlation coefficient of 0.91. This strong correlation indicates that the warmest models in HIST generally exhibit the highest temperature increases under the RCP4.5. Moreover, the models that have no biases in HIST show warming responses in RCP4.5. The highest and lowest temperature responses are typically found in the winter peaks; these temperature changes are 6.5 °C from the model GISS-E2-H and −2.5 °C from IPSL-CM5B-LR. Therefore, the temperature responses of the models are found to be highly sensitive to temperature biases at the four peaks in simulating of the present climate. It implies that these strong inter-model statistical correlations have enough potentiality as an 'observational constraint'. Li *et al.* (2016a, 2016b) suggested that realistic present simulation would lead to a more reliable climate projection and introduced a method to calibrate the model error effects based on an observational constraint of excessive

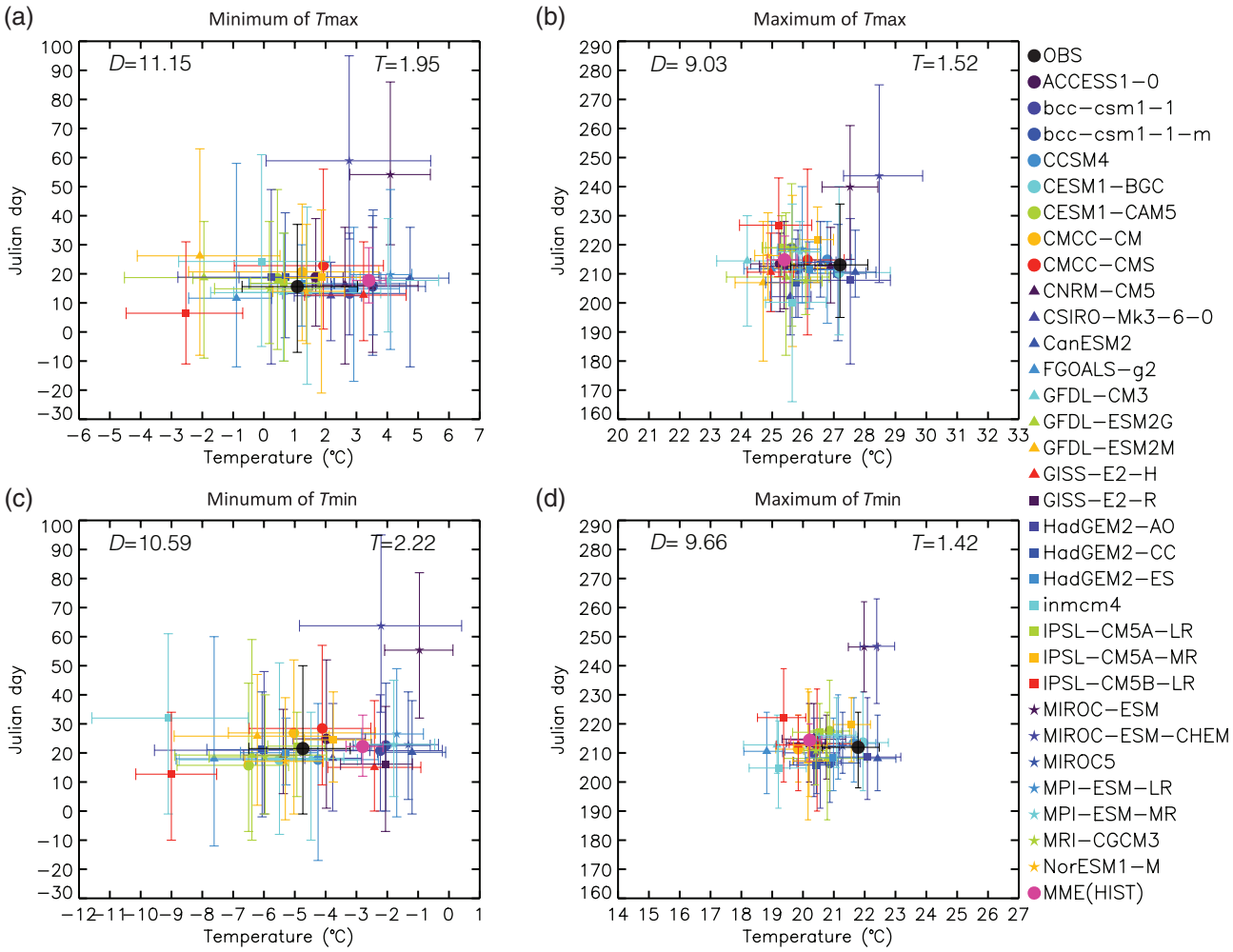

Figure 3. Annual extreme temperatures and their dates of occurrence in observational data (black), MME (pink dot) and models (colour) in HIST. The dots represent the mean temperatures and days of occurrences, and bars denote the variability. Left and right numbers in each panel show standard deviations associated with observations (black dot) for dates and temperatures, respectively. [Colour figure can be viewed at wileyonlinelibrary.com].

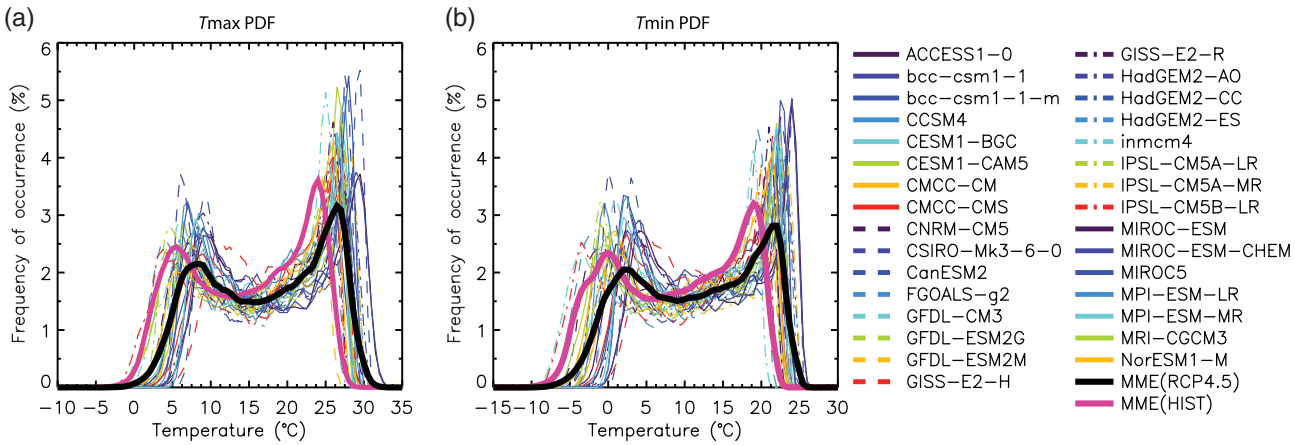

Figure 4. The probability density functions (PDF) for annual daily (a) maximum temperature and (b) minimum temperature over East Asia (100°–150°E, 20°–50°N) for 2075–2099 under RCP4.5. The black and pink curves denote the MMEs under RCP4.5 and HIST, respectively. [Colour figure can be viewed at wileyonlinelibrary.com].

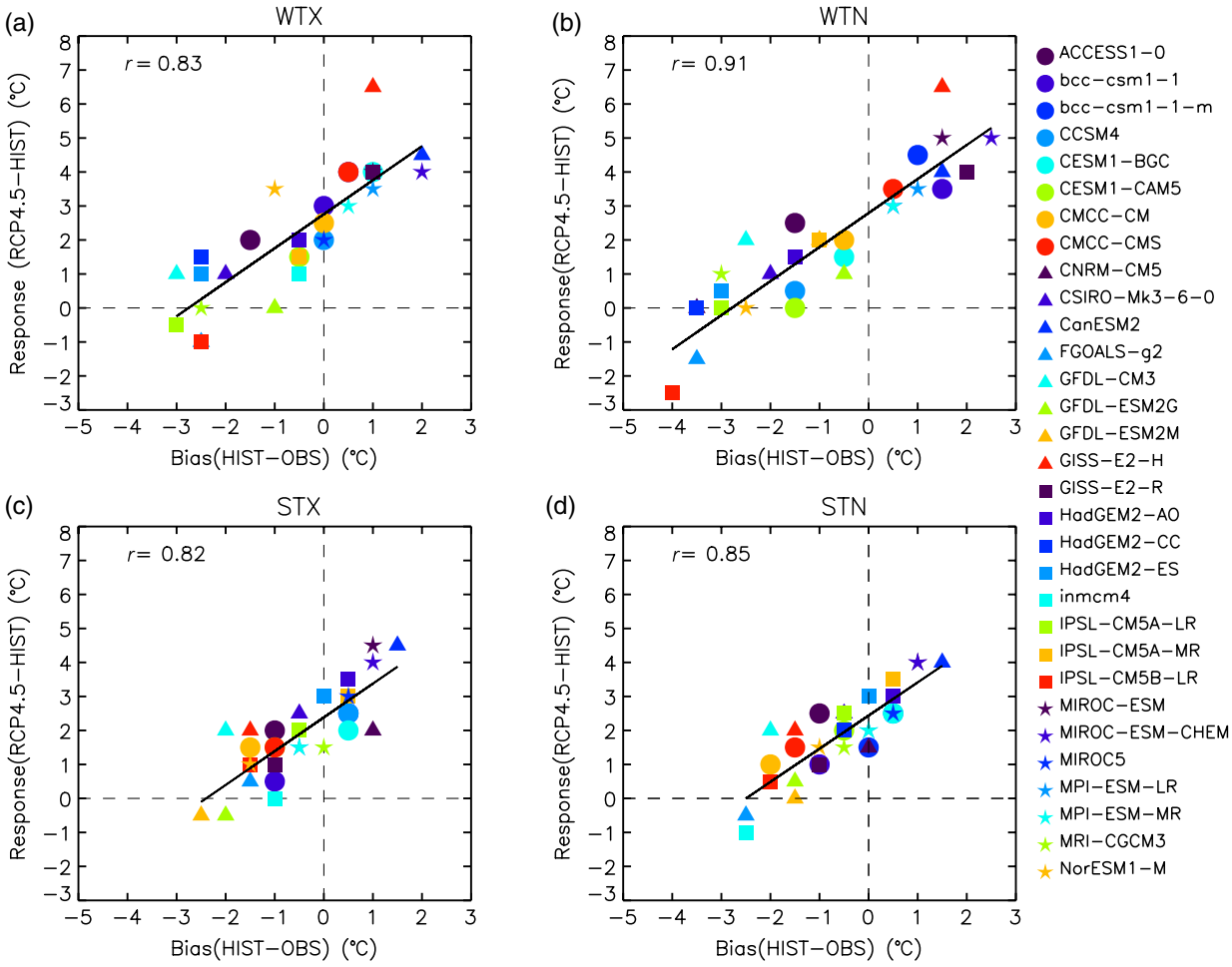

Figure 5. Temperature changes (RCP4.5 minus HIST) of (a) WTX, (b) STX, (c) WTN and (d) STN plotted against biases in present-day projections (HIST minus OBS). [Colour figure can be viewed at wileyonlinelibrary.com].

equatorial cold tongue bias and Indian Ocean Dipole amplitude. Through these previous studies, these results would be contributed to reduce the uncertainty of projection for extreme temperature changes over East Asia and it should be necessary. In addition, we evaluated frequency responses based on the frequency biases of the four peaks (not shown). The responses of frequencies are linearly related to biases in the HIST with high correlation coefficients ranging from 0.51 (in WTX) to 0.72 (in STX). The summer peak frequencies show stronger connections between biases and responses than do the winter peak frequencies. To investigate the relationships between model biases and projected changes in seasonal mean temperatures over East Asia, we performed the same analyses for both summer (June–July–August, JJA) and winter (December–January–February, DJF) mean temperatures (Figure 6). All models show increases in seasonal mean temperatures over East Asia in the future. Most of the models show negative biases in seasonal mean temperature, especially *T*min. Moreover, the winter mean temperature biases are distributed within larger temperature range than those of summer. In particular, MIROC-ESM and MIROC-ESM-CHEM show the largest biases in winter mean temperature due to the shift of annual cycle projection in present. Although the summer mean responses of *T*max tend to have the closet relationship with biases having negative correlation, this relationship is not significant. That is, the changes in seasonal mean temperatures and biases in the HIST show no interrelationships. These findings imply that the projected changes in mean temperatures over East Asia are not dependent upon the performance of the models for the present climate and annual temperature and frequency distributions are more sensitive to biases than are mean temperatures over East Asia (Figure 5).

4.3. Heat-wave probabilities

The broadening of the temperature PDF influences the temperature extremes and the changes of the high value of the daily temperature in summer are related to the changes of the heat-wave characteristics in future climate. To examine the future change of heat-wave characteristics, the probabilities of heat-wave duration and intensity are investigated by comparing MME and BMME in Figure 7. In present climate, short-lasting heat waves occur more frequently and most of heat-wave events persist for less than 10-days in BMME, while MME shows two peaks in duration at about 3–5 days and near 30-days. It implies

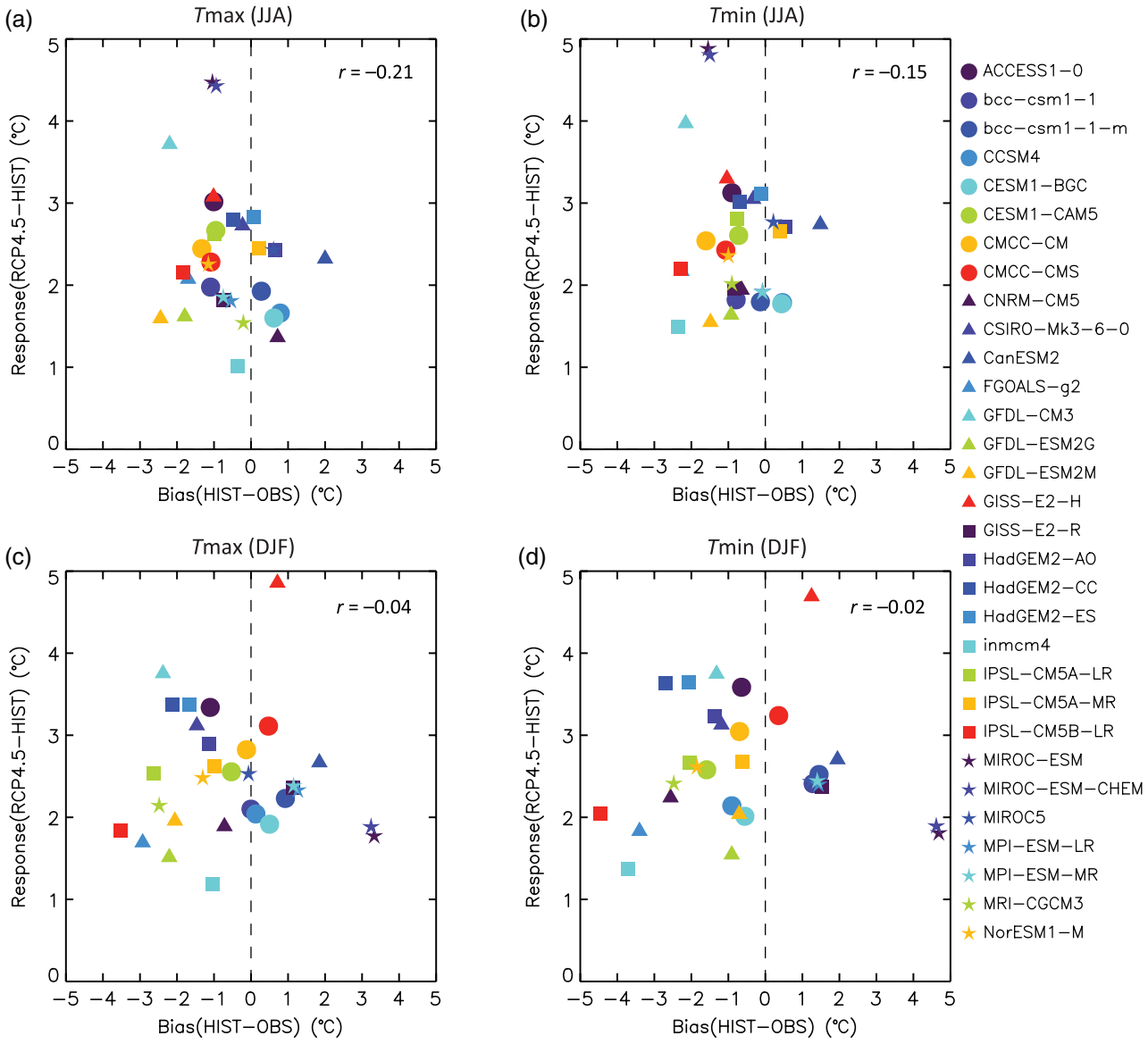

Figure 6. Seasonal means of maximum and minimum temperature changes over East Asia (RCP4.5 minus HIST) plotted against biases in present-day projections (HIST minus OBS) for (a) and (b) JJA and (c) and (d) DJF. [Colour figure can be viewed at wileyonlinelibrary.com].

that the models that reproduce good performance of the simulation in PDFs for the present climate simulate the short-lasting and high-temperature heat-wave events better. This discrepancy of probabilities may be due to accumulated biases from all models. In the future, PDFs of heat-wave duration in MME and BMME show two-peak shapes, which means that the short-lasting heat-wave events will be reduced while long-lasting heat waves will be increased. Namely, heat-wave occurrence frequencies will be decreased and one heat-wave event may persist longer in the future. The peak of heat-wave intensities of BMME is similar to that of MME, while the PDF in BMME is a little broader. In addition, the BMME represents the higher temperature heat-wave events more frequently.

To understand the spatial distribution characteristics of heat waves, the future changes in heat-wave frequency, duration and intensity are examined (Figure 8). The MME and BMME project that the HWF over entire East Asia will be increased and the larger values of the changes in HWF are found over the southern China, particularly coastal regions. The HWF in MME shows the larger increase than those in BMME. On average, the mean values of HWF from MME measures 1.9 and 13.1 larger heat-wave frequencies over the East Asia in HIST and RCP4.5 compare to BMME, respectively (Table 2). That is, the MME simulates more frequent heat-wave events in HIST and RCP4.5 than BMME. Also MME projects large increasing of heat-wave days. The patterns of HWD are similar for HWF, since the number of heat-wave days directly influences events durations. Across most of the East Asia, increases in HWF result in increases of HWD. Indeed, the greatest similarity exists between HWF and HWD, implying that changes in the number of heat-wave events derive the overall number of heat-wave events. Average HWD in MME (BMME) is 14.2 (9.9) days in HIST and 79.9

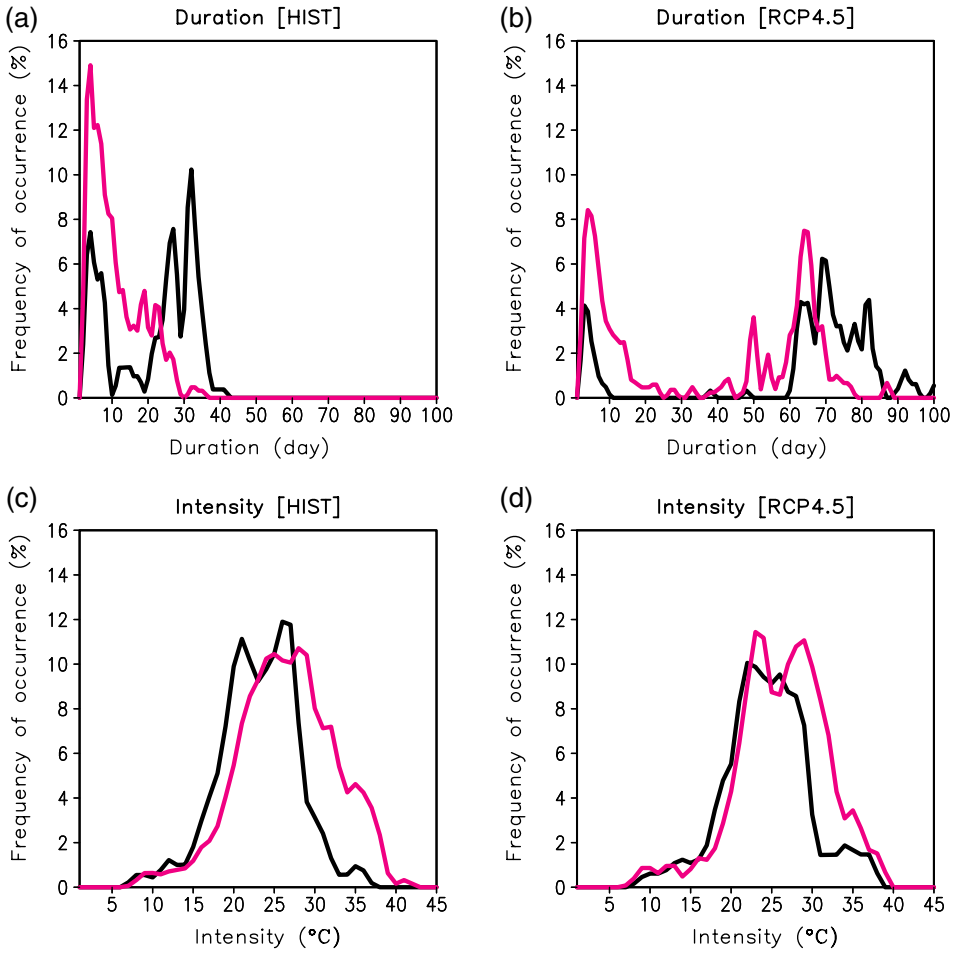

Figure 7. The probability density functions (PDFs) for heat-wave durations and intensities. (a)–(c) represent the PDFs in HIST and (b)–(d) show the PDFs in RCP4.5. The black and pink curves denote the MMEs and BMMEs, respectively. [Colour figure can be viewed at wileyonlinelibrary .com].

(54.4) days in RCP4.5, with 65.5 (44.5) days increasing. Therefore, BMME projects heat wave less frequently and shorter than MME. In contrast with HWF and HWD, the spatial patterns of future changes in HWA from MME and BMME show similar magnitude each other. Although the changes in average HWA of MME are similar to that of BMME with 2.1 and 2.2 °C, the temperature values of hottest day of hottest yearly event in BMME is about approximately 4.1–4.2 °C higher than that of MME. Consequently, BMME simulates the hotter extreme temperature than MME, which is implied the broadening of the temperature PDF toward higher temperature.

5. Conclusions

We have presented an assessment of probabilistic extreme temperatures and their projected future changes based on CMIP5 model simulations for East Asia. Daily *T*max, *T*min and the probability distributions of these variables are closely related to changes in extreme temperature events. Thirty-one CMIP5 models were used for simulations that focused on the historical period 1979–2005. We compared the distributions of daily *T*max and *T*min of the model simulation outputs with those of observations and used PDFs to identify potential differences between these two datasets. Most models effectively simulated both the shapes of the observed PDFs for daily *T*max and *T*min and the temperatures of the warm- and cold-season peaks. The models simulate the frequency distribution of *T*max more accurately than that of *T*min, and exhibit large discrepancies between individual models among 31 models simulations for simulating the frequency of each peak, especially for *T*min. Overall, the CMIP5 models effectively captured the shapes of the corresponding observation-based PDFs and annual distributions for the present-day *T*max and *T*min over East Asia. Based on the skill scores calculated as the sum of the distances between modelled results and observation-based results at the four extreme temperature peaks in PDFs and pattern correlation, it is notable that the CMIP5 models reproduce the annual distributions of present-day *T*max and *T*min over East Asia reasonably well. In addition, we investigate the occurrence dates and temperatures of annual extreme events of *T*max and *T*min in the present climate. The extreme events were calculated based on the maxima and minima of extreme temperatures and theirs dates of occurrence. For all extreme events, the variability of dates is about 10 days and the variability of temperatures is about 2 °C. Moreover, the minimum

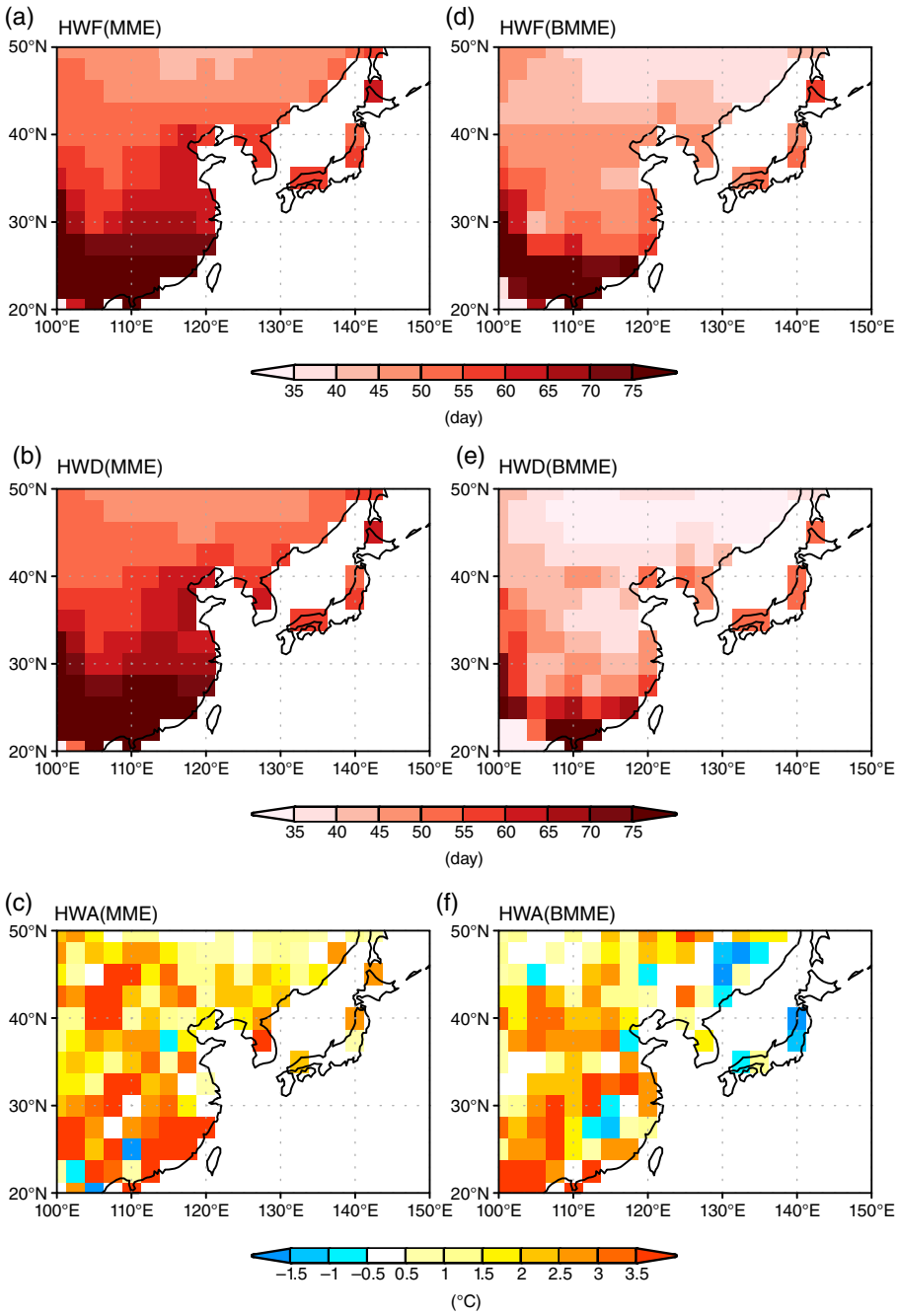

Figure 8. Future changes of heat-wave indices; (a) HWF (yearly sum of participating heat-wave days), (b) HWD (length of the longest yearly events), and (c) HWA (hottest day of hottest yearly events) for MME. (d)–(f) Same as (a)–(c) but for BMME. [Colour figure can be viewed at wileyonlinelibrary.com].

extreme events are more dependent to models than maximum extreme events.

For the future period 2075–2099 under the RCP4.5 scenario, the shapes of the model PDFs for *T*max and *T*min show broadening in the shape of PDFs for HIST. All models exhibit horizontal shifting by 2.0 to 3.0 °C at the four peaks. The relationship between temperature biases of dominant two peaks in PDFs and temperature responses are investigated. The temperature changes and biases show linear relationships with high correlation coefficients, thus, model projections of future changes in PDFs are affected by biases in projecting present extreme temperatures. The

Table 2. The mean values of heat-wave indices over the East Asia in HIST (1979–2005) and RCP4.5 (2075–2099) scenarios.

		HIST	RCP4.5	DIFF (RCP4.5 minus HIST)
HWF	MME	17.3	81.0	63.7
	BMME	15.4	67.9	52.5
HWD	MME	14.2	79.7	65.5
	BMME	9.9	54.4	44.5
HWA	MME	22.6	24.7	2.1
	BMME	26.4	28.6	2.2

projected temperature frequencies and responses are linearly related to biases in HIST with high correlation coefficients. In particular, the models that have warm biases in HIST generally exhibit larger temperature increases under RCP4.5. However, the relationships between future changes in seasonal mean temperature and biases in HIST for East Asia have no correlations, especially for the winter. Namely changes in temperature and frequency distributions are more sensitive to model performance for the present climate than changes in mean temperature. Therefore, improving the simulation skill of models for annual distribution is necessary to improve predictions and understanding of future climate changes in East Asia. In addition, we suggest the future changes in probabilities of heat wave as one of extreme temperature events by comparing between MME and BMME. In terms of heat-wave duration BMME represents concentration of short-lasting heave wave events in present climate. The BMME also shows the higher temperature heat-wave events more frequently in present and future. In spatial distribution, both of MME and BMME simulate increases of heat-wave frequency and duration and MME tends to overestimate. The intensity of heat wave increase about 2 °C in the future for both of MME and BMME, but BMME has about 4 °C higher temperature values than MME since the MME involves all models with cold and warm biases.

Apart from statistical relationships between extreme temperature biases and response under global climate change, it is also important to focus on the physical explanations of these results. In addition, the frequency and duration of heatwaves and extreme drought, rather than the probabilistic changes in this study, will need to be further considered and examined.

Acknowledgements

This study was financially supported by the GRL grant of the National Research Foundation (NRF) funded by the Korean Government (MEST 2011-0021927). YWS was supported by NRF-2015-Fostering Core Leaders of the Future Basic Science Program/Global Ph.D. Fellowship Program (2015H1A2A1034717) and JYL was supported by the National Research Foundation (NRF-2015 R1C1A2A01053980) in Korea. KSY and YWS were supported by NRF-2015R1C1A1A01054992.

References

Andronova NG, Schlesinger ME. 2001. Objective estimation of the probability density function for climate sensitivity. *J. Geophys. Res.* **106**(D19): 22605–22611.

Boberg F, Berg P, Thejll P, Gutowski WJ, Christensen JH. 2009. Improved confidence in climate change projections of precipitation evaluated using daily statics form the PRUDENCE ensemble. *Clim. Dyn.* **32**: 1097–1106.

Cattiaux J, Douville H, Peings Y. 2013. European temperatures in CMIP5: origins of present-day biases and future uncertainties. *Clim. Dyn.* **41**: 2889–2907.

Coumou D, Robinson A, Rahmstorf S. 2013. Global increase in record breaking monthly-mean temperatures. *Clim. Chang.* **117**: 771–782.

Dessai S, Lu X, Hulme M. 2005. Limited sensitivity analysis of regional climate change probabilities for the 21st century. *J. Geophys. Res.* **110**: D19108. https://doi.org/10.1029/2005JD005919.

Donat MG, Alexander LV. 2012. The shifting probability distribution of global daytime and night-time temperatures. *Geophys. Res. Lett.* **39**: L14707. https://doi.org/10.1029/2012GL052459.

Easterling DF, Meehl GA, Parmesan C, Changnon SA, Karl TR, Mearns LO. 2000. Climate extremes: observations, modeling, and impacts. *Science* **289**: 2068–2074.

Fischer EM, Schär S. 2010. Consistent geographical patterns of changes in high-impact European heatwaves. *Nat. Geosci.* **3**: 398–403. https://doi.org/10.1038/ngeo866.

Forest CE, Stone PH, Sokolov AP, Allen MR, Webster MD. 2002. Quantifying uncertainties in climate system properties with the use of recent climate observations. *Science* **295**: 113–117.

Ha KJ, Yun KS. 2012. Climate change effects on tropical night days in Seoul, Korea. *Theor. Appl. Climatol.* **109**: 191–203. https://doi.org/10.1007/s00704-011-0573-y.

Held IM, Soden BJ. 2006. Robust responses of the hydrological cycle to global warming. *J. Clim.* **19**: 5686–5699.

Huang P, Xie SP, Hu K, Huang G, Huang R. 2013. Patterns of the seasonal response of tropical rainfall to global warming. *Nat. Geosci*. **6**(5): 357–361.

Kanamitsu M et al. 2002. NCEP-DOE AMIP-II reanalysis (R-2). *Bull. Am. Meteorol. Soc.* **83**: 1631–1643.

Kharin VV, Zwiers FW, Zhnag X, Hegerl GC. 2007. Changes in temperature and precipitation extremes in the IPCC ensemble of global coupled model simulations. *J. Clim.* **20**: 1419–1444.

Kharin VV, Zwiers FW, Zhang X, Wehner M. 2013. Changes in temperature and precipitation extremes in the CMIP5 ensemble. *Clim. Chang.* **119**: 345–357.

Knutti R, Stocker TF, Joos F, Plattner GK. 2002. Constraints on radiative forcing and future climate change from observations and climate model ensembles. *Nature* **416**: 719–723.

Li G, Xi SP, Du Y. 2016a. A robust but spurious pattern of climate change in model projections over the tropical Indian Ocean. *J. Clim.* **29**: 5589–5608.

Li G, Xi SP, Du Y, Luo Y. 2016b. Effects of excessive equatorial cold tongue bias on the projections of tropical Pacific climate change. Part I: the warming pattern in CMIP5 multi-model ensemble. *Clim. Dyn.* **47**: 3817–3831.

Masanganise J, Magodora M, Mapuwei T, Basira K. 2014. An assessment of CMIP5 global climate model performance using probability density functions and a match metric method. *Sci. Insights Int. J.* **4**(1): 1–8.

Matsueda M, Palmer TN. 2011. Accuracy of climate change predictions using high resolution simulations as surrogates of truth. *Geophys. Res. Lett*. **38**: L05803. https://doi.org/10.1029/2010GL046618.

Min S, Zhang X, Zwiers F, Shiagama H, Tung YS, Wehner M. 2013. Multimodel detection and attribution of extreme temperature changes. *J. Clim.* **26**: 7430–7451.

Nairn J, Fawcett R. 2015. The excess heat factor: a metric for heatwave intensity and its use in classifying heatwave severity. *Int. J. Environ. Res. Public Health* **12**: 227–253.

Nairn J, Fawcett R, Ray D. 2009. Understanding high impact weather, CAWCR modelling workshop. Bureau of Meteorology; Melbourne, Australia: Defining and predicting excessive heat events, a national system.

Perkins SE, Alexander LV. 2012. On the measurement of heat waves. *J. Clim.* **26**: 4500–4517.

Perkins SE, Pitman AJ. 2009. Do weak AR4 models bias projections of future climate changes over Australia? *Clim. Chang.* **93**: 527–558.

Perkins SE, Pitman AJ, Holbrook NJ, McAneney J. 2007. Evaluation of the AR4 climate models' simulated daily maximum temperature, minimum temperature, and precipitation over Australia using probability density functions. *J. Clim.* **20**: 4356–4376.

Rohini P, Rajeevan M, Srivastava AK. 2016. On the variability and increasing trends of heat waves over India. *Sci Rep* **6**: 26153. https://doi.org/10.1038/srep26153.

Scheff J, Frierson DMW. 2012. Robust future precipitation declines in CMIP5 largely reflect the poleward expansion of model subtropical dry zones. *Geophys. Res. Lett*. **39**: L18704. https://doi.org/10.1029/2012GL052910.

Seo YW, Kim H, Yun KS, Lee JY, Ha KH, Moon JY. 2014. Future change of extreme temperature climate indices over East Asia with uncertainties estimation in the CMIP5. *Asia-Pac. J. Atmos. Sci.* **50**: 57–72.

Sillmann J, Kharin VV, Zhang X, Zwiers FW, Bronaugh D. 2013a. Climate extremes indices in the CMIP5 multimodel ensemble:part 1.

Model evaluation in the present climate. *J. Geophys. Res. Atmos.* **118**: 1–18. https://doi.org/10.1002/jgrd.50203.

Sillmann J, Kharin VV, Zwiers FW, Zhang X, Bronaugh D. 2013b. Climate extremes indices in the CMIP5 multimodel ensemble: part 2. Future climate projection. *J. Geophys. Res. Atmos.* **118**: 2473–2493. https://doi.org/10.1002/jgrd.50188.

Sun Q, Miao C, Duan Q. 2015. Comparative analysis of CMIP3 and CMIP5 global climate models for simulating the daily mean, maximum, and minimum temperatures and daily precipitation over China. *J. Geophys. Res. Atmos.* **120**: 4806–4824. https://doi.org/10.1002/2014JD022994.

Tebaldi C, Hayhoe K, Arblaster JM, Meehl GA. 2006. Going to the extremes: an intercomparison of model-simulated historical and future changes in extreme events. *Clim. Chang.* **79**: 185–211.

Wang L, Chen W. 2014. A CMIP5 multimodel projection of future temperature, precipitation, and climatological drought in China. *Int. J. Climatol.* **35**: 2059–2078.

Watterson IG. 2008. Calculation of probability density functions for temperature and precipitation change under global warming. *J. Geophys. Res.* **113**: D12106. https://doi.org/10.1029/2007JD009254.

Yun KS, Shin SH, Ha KJ, Kitoh A, Kusunoki S. 2008. East Asian precipitation change in the global warming climate simulated by a 20-km mesh AGCM. *Asia-Pac. J. Atmos. Sci.* **44**: 233–247.

Zwiers FW, Zhang X, Feng Y. 2011. Anthropogenic influence on long return period daily temperature extremes at regional scales. *J. Clim.* **24**: 881–892.

